

## VERTICAL RELAXATION OF A MOONLET PROPELLER IN SATURN'S A RING

H. HOFFMANN, M. SEIß, AND F. SPAHN

Institute of Physics and Astronomy, University of Potsdam, D-14476 Golm, Germany  
 Received 2012 December 10; accepted 2013 January 25; published 2013 February 11

### ABSTRACT

Two images, taken by the *Cassini* spacecraft near Saturn's equinox in 2009 August, show the Earhart propeller casting a 350 km long shadow, offering the opportunity to watch how the ring height, excited by the propeller moonlet, relaxes to an equilibrium state. From the shape of the shadow cast and a model of the azimuthal propeller height relaxation, we determine the exponential cooling constant of this process to be  $\lambda = 0.07 \pm 0.02 \text{ km}^{-1}$ , and thereby determine the collision frequency of the ring particles in the vertically excited region of the propeller to be  $\omega_c/\Omega = 0.9 \pm 0.2$ .

**Key words:** planets and satellites: individual (Saturn) – planets and satellites: rings

### 1. INTRODUCTION

Small moonlets in Saturn's A ring, not large enough to open circumferential gaps like the ring moons Pan and Daphnis, induce S-shaped structures in the surrounding ring material (Spahn & Sremčević 2000; Sremčević et al. 2002; Seiß et al. 2005; Sremčević et al. 2007; Lewis & Stewart 2009). More than 150 of these *propeller* structures have been found in images taken by the *Cassini* spacecraft (Tiscareno et al. 2006, 2008). Although most propellers have been identified in the radial region between 126,750 km and 132,000 km in the mid A ring, very large propellers with a few kilometers of radial extent and up to several hundred kilometers of azimuthal length were detected in the region between the Encke and Keeler gaps, pointing to subkilometer moonlets. These propellers, nicknamed after famous aviators (e.g., Blériot, Earhart, Santos-Dumont), are large enough to be seen on several snapshots taken by *Cassini*'s cameras at different times, confirming their orbital motion (Tiscareno et al. 2010). Properties and evolution of these giant propellers might also be of interest for the growth of planetary embryos in protoplanetary disks (Burns & Cuzzi 2006).

Images taken by *Cassini* around Saturn's equinox in 2009 August (the Sunset at Saturn's rings) show long shadows cast by propellers, offering the opportunity to study their vertical structure. Tiscareno et al. (2010) measured the height of four propellers orbiting between the Encke and Keeler gaps. The Earhart propeller has a height of 260 m, for example. In this Letter, we consider the azimuthal relaxation of this vertical excitation. Two images of the giant propeller Earhart, taken two days after equinox, show a 350 km long,<sup>1</sup> pronounced shadow (see Figure 1(a)). Assuming the propeller height to vertically limit the light blocking region of the propeller, we estimate the boundaries of the cast shadows using a model of the azimuthal relaxation of the propeller height. Matching the model to the observed shadows in the two Earhart images, we determine the exponential cooling constant of Earhart's height relaxation and thereby directly estimate the collision frequency of the ring particles in the vertically excited region.

### 2. AZIMUTHAL PROPELLER HEIGHT RELAXATION

The encounter of the ring particles with the propeller moonlet results in an increased ring thickness, which subsequently relaxes back to the thickness of an unperturbed ring. We consider the disturbed balance of viscous heating and collisional cooling as the main mechanism of this relaxation. The related local energy balance of the ring particle's random motion is given by

$$\frac{dE_{\text{kin}}}{dt} = \frac{9}{4} \nu \Omega^2 - \frac{\omega_c}{3} (1 - \varepsilon^2) E_{\text{kin}}, \quad (1)$$

with the specific energy  $E_{\text{kin}} = c^2/2$  and the mean random velocity  $c = (c_x^2 + c_y^2 + c_z^2)^{1/2}$  of the ring particles (Morishima & Salo 2006; Schmidt et al. 2009). The first term on the right hand side describes the energy gain due to viscous heating (at the expense of the mean Keplerian ring motion), with  $\nu$  being the kinematic viscosity and  $\Omega$  the Keplerian angular velocity. The second term describes the average energy dissipation due to inelastic collisions between ring particles (granular cooling), with  $\varepsilon$  being the normal coefficient of restitution and  $\omega_c$  the collision frequency of the ring particles.

For the quantitative description of the relaxation process we assume a local Cartesian coordinate system, corotating with and centered on the moonlet, with a radial distance of  $x = r - a_{\text{moon}}$  from the moonlet and azimuthal coordinate  $y$ . By assuming a stationary process, we express the time dependence through the azimuthal length  $y = a(\Omega - \Omega_{\text{moon}})t \approx -3\Omega_{\text{moon}}xt/2$ , where the frequency  $\Omega(r)$  is linearly expanded around the moonlet location. We are interested in the evolution of the propeller height downstream of the moonlet, which is in direction of increasing  $y$  values for  $x < 0$  and decreasing  $y$  values for  $x > 0$  in the corotating frame.

We apply a viscosity of the form  $\nu = \nu_0(\tau) + \beta(\tau)c^2 = \nu_0(\tau) + 2\beta(\tau)E_{\text{kin}}$  (Schmidt et al. 2009), where the first term corresponds to the contribution to the viscosity which is not affected by the velocity dispersion  $c^2 = 2E_{\text{kin}}$  (nonlocal viscosity), while the second term considers the effect of  $E_{\text{kin}}$  (local contribution). This leads to a  $c^2$ - (and thus  $E_{\text{kin}}$ -) dependent viscous heating term in Equation (1). Additionally assuming the normal coefficient of restitution  $\varepsilon$  to be constant, the solution of Equation (1) then reads

$$E_{\text{kin}}(|y|) = (E_{\text{max}} - E_0) \exp(-\lambda|y|) + E_0, \quad (2)$$

<sup>1</sup> As reported by the Cassini ISS team on their Web site (PIA 11672). This value agrees well with our measurements.

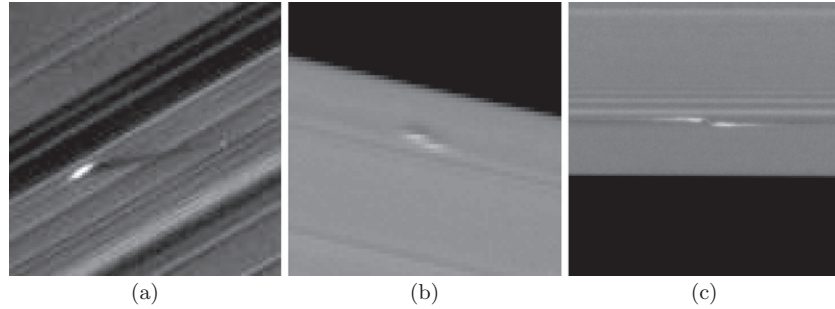


**Figure 1.** Different views of the Earhart propeller taken by *Cassini*'s narrow angle camera. (a) was taken two days after Saturn's equinox on 2009 August 13. The resolution is  $7 \text{ km pixel}^{-1}$  or projected onto the ring plane, the azimuthal resolution is about  $15\text{--}16 \text{ km pixel}^{-1}$  (radial resolution is about  $14 \text{ km pixel}^{-1}$ ). Earhart casts a 350 km long, pronounced shadow. (b) shows Earhart in 2009 May, casting a shadow not nearly as pronounced as in August. (c) shows the typical S-shaped structure induced by the moonlet and was taken on 2008 April 11. Image numbers are (a) N1628846513, (b) N1621959753, and (c) N1586628622.

with the exponential cooling constant

$$\lambda = \frac{2\omega_c(1 - \varepsilon^2)}{9\Omega|x|} - \frac{3\beta\Omega}{|x|}. \quad (3)$$

We have further assumed an azimuthally constant optical depth  $\tau$  for the perturbed region (after the encounter with the moonlet), which is reasonable for large propellers like Earhart, because the timescale of the height decay is small compared to the large diffusive timescales responsible for the gap closing (Sremčević et al. 2002).

We use half the ring thickness as propeller height and assume  $z$  independent components of the mean random velocity  $c_x$ ,  $c_y$ , and  $c_z$  (cf. Simon & Jenkins 1994; Schmidt et al. 1999). The propeller height is then proportional to  $c_z/\Omega$  (Stewart et al. 1984). Because the asymptotic ratios of the mean random velocities  $(c_y/c_x)_{\text{eq}}$  and  $(c_z/c_x)_{\text{eq}}$  are established after only a few collisions per particle (Hämeen-Anttila & Lukkari 1980; Hämeen-Anttila & Salo 1993) after the moonlet scattering, we regard  $c^2$  (and therefore  $E_{\text{kin}}$ ) as a function of only one of the components  $c_x$ ,  $c_y$ ,  $c_z$ , for example

$$c^2 = c_x^2 \{1 + (c_y/c_x)_{\text{eq}}^2 + (c_z/c_x)_{\text{eq}}^2\}. \quad (4)$$

Using  $c_z = (c_z/c_x)_{\text{eq}} \cdot c_x$  and  $c^2 = 2E_{\text{kin}}$ , we express  $c_z$  as a function of the specific random energy  $E_{\text{kin}}$

$$c_z(E_{\text{kin}}) = \left(\frac{c_z}{c_x}\right)_{\text{eq}} \sqrt{\frac{2}{1 + (c_y/c_x)_{\text{eq}}^2 + (c_z/c_x)_{\text{eq}}^2}} E_{\text{kin}}. \quad (5)$$

The propeller height is then given by  $H = \alpha\sqrt{E_{\text{kin}}}$ . Although the exact value of  $\alpha$  is not needed for our purposes, a typical value would be  $\alpha = 1.23/\Omega$ , where we use the effective geometric thickness of the ring (Schmidt et al. 2009) and  $(c_y/c_x)_{\text{eq}} = 0.5$  and  $(c_z/c_x)_{\text{eq}} = 0.65$  (cf. Goldreich & Tremaine 1978; Salo 1995). With  $H_{\text{max}} = \alpha\sqrt{E_{\text{max}}}$  and  $H_0 = \alpha\sqrt{E_0}$  the azimuthal evolution of the propeller height becomes

$$H(y) = \sqrt{(H_{\text{max}}^2 - H_0^2) \exp(-\lambda y) + H_0^2}. \quad (6)$$

### 3. OBSERVATIONS

On 2009 August 13 *Cassini* took two images showing the Earhart propeller, orbiting near the Encke gap, casting a 350 km long, pronounced shadow (shown in Figure 1(a)). The elevation angle of the sun was  $0^\circ 035'$ , so that the incoming sunlight was nearly parallel to the ring plane. In the local corotating frame

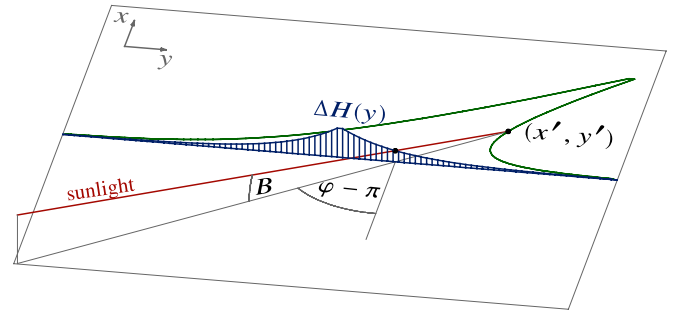


**Figure 2.** Calculation of the shadow boundary by projecting the height difference  $\Delta H(y)$  between propeller and surrounding ring material onto the ring plane, using the elevation angle of the sunlight  $B$  and the longitude of the sun  $\varphi$ .

$(x, y)$  centered on the propeller moonlet the longitude of the sun was  $230^\circ$ . These images are unique in that (1) they show a very pronounced cast shadow and (2) Earhart is an often imaged and thus well known giant propeller. The resolution of Figure 1(a) is  $7 \text{ km pixel}^{-1}$ , resulting in a projected azimuthal ring plane resolution of about  $15\text{--}16 \text{ km pixel}^{-1}$ —providing a fairly good resolution for our purposes.

By assuming the azimuthal evolution of the propeller height to vertically limit the light blocking region of the propeller (see Figure 2), we determine the exponential cooling constant  $\lambda$  of the propeller height from the shape of the shadow cast by Earhart. We project the height difference between the propeller and the surrounding ring material  $\Delta H(y) = H(y) - H_{\text{eq}}$  onto the ring plane to estimate the shadow boundary

$$\begin{aligned} x'(y) &= \Delta H(y) \cot(B) \cos(\varphi - \pi) \\ y'(y) &= y + \Delta H(y) \cot(B) \sin(\varphi - \pi), \end{aligned} \quad (7)$$

where  $B$  is the elevation angle of the sunlight and  $\varphi$ , measured from the  $x$ -axis toward the  $y$ -axis, the longitude of the sun in a frame corotating with and centered on the moonlet.

Figure 3 shows the two magnified and reprojected near equinox images of Earhart, where Earhart's orbital motion is to the right and the direction toward Saturn is down. From the shadow length of 350 km, we determine  $\Delta H_{\text{max}}$  to be 215 m. Varying the exponential cooling constant  $\lambda$ , we visually find the best match between projected curve and shadow boundary for  $\lambda = 0.07 \pm 0.02 \text{ km}^{-1}$ , leading to a propeller height halving after about 20 km. Although strictly  $H_{\text{eq}} \neq H_0$ , the influence of the difference was negligible, so we set them equal and found values of a few tens of meters to be consistent with our visually fitted curves. We measured the azimuthal length of the bright propeller

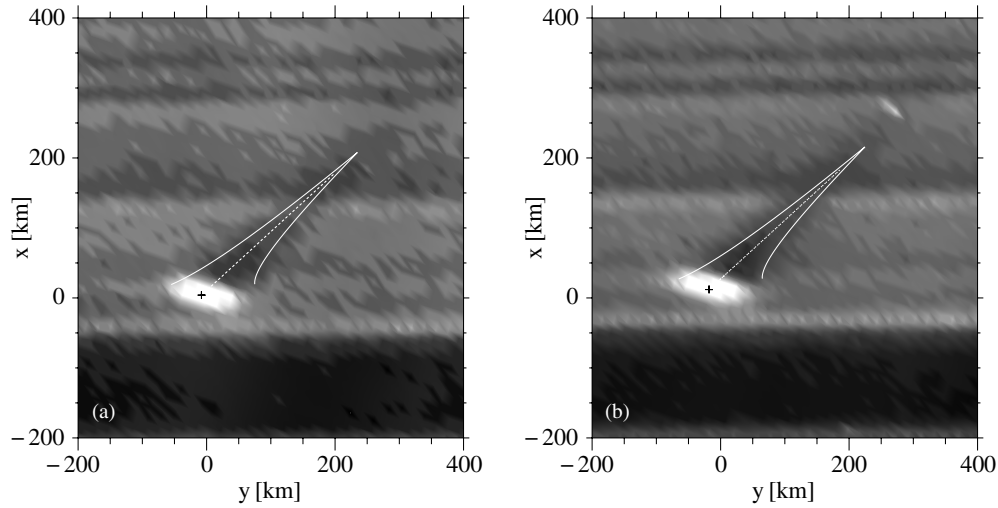


**Figure 3.** Two near equinox images of Earhart magnified and reprojected. Direction toward Saturn is down and the orbital motion of Earhart is to the right. The azimuthal evolution of the height difference between propeller and surrounding ring material is projected into the image as an estimate of the shadow boundary using Equation (7). The beginning and end of the projected curve correspond to the azimuthal length of the bright propeller region. We find the exponential cooling constant to be  $\lambda = 0.07 \pm 0.02 \text{ km}^{-1}$  and find thereby a collision frequency of  $\omega_c/\Omega = 0.9 \pm 0.2$  in the vertically excited region, corresponding to 5–6 collisions per particle per orbit. Image numbers are (a) N1628846480 and (b) N1628846513.

region in Figure 1(a) to be  $120 \pm 20 \text{ km}$ .<sup>2</sup> This azimuthal length corresponds to a decay of the propeller height (downstream) to about 15% of the initial value and confines the shadow casting region of the propeller.

From test particle simulations, we expect the largest excitation in the propeller gap region ( $1.5 h \leq |x| \leq 4 h$ ),<sup>3</sup> with half the optical depth of the unperturbed ring  $\tau = \tau_0/2 = 0.25$ . From observations (Porco et al. 2008) and simulations (Salo et al. 2004) we know the effective normal coefficient of restitution to be in the range 0.1–0.5 and by identifying the  $c^2$ -dependent part of the viscosity with that of Goldreich & Tremaine (1978), we find

$$\beta(\tau) = \frac{k_1 \tau}{\Omega(1 + \tau^2)}. \quad (8)$$

With  $k_1 = 0.15$  (Stewart et al. 1984) and for the middle of the gap region at  $|x| = 2.5 h$ , where we used  $h = 370 \text{ m}$  (explained in detail in an upcoming paper), we find a collision frequency of  $\omega_c/\Omega = 0.9 \pm 0.2$ ,<sup>4</sup> corresponding to 5–6 collisions per particle per orbit. To put this value into perspective, an often used estimate of the collision frequency for dilute rings, not perturbed by a propeller moonlet, is  $\omega_c = 3\Omega\tau$  (cf. Schmidt et al. 2009; Shu & Stewart 1985), giving  $\omega_c/\Omega = 0.75$  or about 5 collisions per particle per orbit for  $\tau = 0.25$ . N-body simulations of planetary rings, excluding self-gravity, are in good agreement with this formula, whereas, in simulations including self-gravity, the collision frequency can be up to three times larger (Salo 1995; Salo et al. 2001).

A detailed description of the disturbed balance of viscous heating and collisional cooling might be more complicated and worthwhile to be treated by proper kinetics in the future, but our simple modeling of the azimuthal height relaxation based solely on the disturbed balance of viscous heating and granular

cooling already enables a good explanation of the 2009 equinox images of Earhart and can well be used as starting reference for more comprehensive theories in the future.

We kindly acknowledge the efforts of the Cassini ISS team in the design and operation of the ISS instrument. We thank P. Nicholson for his helpful comments. This work was supported by Deutsche Forschungsgemeinschaft (Sp 384/24-1; 25-1).

## REFERENCES

- Burns, J. A., & Cuzzi, J. N. 2006, *Sci*, 312, 1753  
 Goldreich, P., & Tremaine, S. 1978, *Icar*, 34, 227  
 Hämeen-Anttila, K. A., & Lukkari, J. 1980, *Ap&SS*, 71, 475  
 Hämeen-Anttila, K. A., & Salo, H. 1993, *EM&P*, 62, 47  
 Lewis, M. C., & Stewart, G. R. 2009, *Icar*, 199, 387  
 Morishima, R., & Salo, H. 2006, *Icar*, 181, 272  
 Porco, C. C., Weiss, J. W., Richardson, D. C., et al. 2008, *AJ*, 136, 2172  
 Salo, H. 1995, *Icar*, 117, 287  
 Salo, H., Karjalainen, R., & French, R. G. 2004, *Icar*, 170, 70  
 Salo, H., Schmidt, J., & Spahn, F. 2001, *Icar*, 153, 295  
 Schmidt, J., Ohtsuki, K., Rappaport, N., Salo, H., & Spahn, F. 2009, in *Saturn from Cassini-Huygens*, ed. M. K. Doherty et al. (Dordrecht: Springer), 413  
 Schmidt, J., Salo, H., Petzschmann, O., & Spahn, F. 1999, *A&A*, 345, 646  
 Seiß, M., Spahn, F., Sremčević, M., & Salo, H. 2005, *GeoRL*, 32, L11205  
 Shu, F. H., & Stewart, G. R. 1985, *Icar*, 62, 360  
 Simon, V., & Jenkins, J. T. 1994, *Icar*, 110, 109  
 Spahn, F., & Sremčević, M. 2000, *A&A*, 358, 368  
 Sremčević, M., Schmidt, J., Salo, H., et al. 2007, *Natur*, 449, 1019  
 Sremčević, M., Spahn, F., & Duschl, W. J. 2002, *MNRAS*, 337, 1139  
 Stewart, G. R., Lin, D. N. C., & Bodenheimer, P. 1984, in *Planetary Rings*, ed. R. Greenberg & A. Brahic (Tucson, AZ: Univ. of Arizona Press), 447  
 Tiscareno, M. S., Burns, J. A., Hedman, M. M., et al. 2006, *Natur*, 440, 648  
 Tiscareno, M. S., Burns, J. A., Hedman, M. M., & Porco, C. C. 2008, *AJ*, 135, 1083  
 Tiscareno, M. S., Burns, J. A., Sremčević, M., et al. 2010, *ApJL*, 718, L92

<sup>2</sup> A value of 130 km is reported by the Cassini ISS team on their Web site (PIA 11672).

<sup>3</sup> With the Hill radius  $h = a_{\text{moon}}(M_{\text{moon}}/3(M_{\text{moon}} + M_{\text{saturn}}))^{1/3}$  of the propeller moonlet.

<sup>4</sup> To see the influence of the assumed  $c^2$ -dependent viscosity: a neglect of the second term in Equation (3), appropriate for a  $c^2$ -independent viscosity, leads to  $\omega_c/\Omega = 0.35 \pm 0.15$ .